Dispersing and Functionalizing Multiwalled Carbon Nanotubes in TiO_2 Sol

Xing-bin Yan,* Beng Kang Tay, and Yi Yang

School of Electrical and Electronic Engineering, Nanyang Technological University, Singapore 639798

Received: August 22, 2006; In Final Form: October 24, 2006

We report that oxidized multiwalled carbon nanotubes (MWCNTs) can be synchronously dispersed and functionalized in TiO_2 sol via an in situ sol−gel process. Transmission electron microscopy (TEM), X-ray photoelectron spectroscopy (XPS), Raman spectroscopy, and atomic force microscopy (AFM) were used to characterize the functionalized MWCNTs. The results revealed that the hydrolysis and condensation originated from $Ti(OC_4H_9)_4$ molecules favor the dispersion of MWCNTs in as-prepared TiO_2 sol. Based on the strong interaction between the oxidized MWCNTs and TiO_2 sol during the in situ sol−gel process, MWCNT (core)−TiO_x (shell) tubular composites and TiO_2 nanotubes can be obtained through filtrating, washing, and annealing of this kind of TiO_2 sol containing functionalized MWCNTs, as revealed by TEM, XPS, Raman spectroscopy, and redispersion experiment. By casting the dilute dispersion of functionalized MWCNTs onto a hydrophilic Si surface, discrete and individual nanotubes can be observed by AFM.

Introduction

Carbon nanotubes (CNTs), due to their extraordinary properties such as excellent Young's modulus, good flexibility, and high electrical and thermal conductivity, are recognized as reinforcement for high-performance, multifunctional composites.[1] Recently, there have been considerable achievements in CNT−polymer composites, which show a remarkable enhancement in electrical and mechanical properties compared to monolithic polymers.[2−6] It is well-known that ceramics have high stiffness and thermal stability, but relatively low breaking strengths. Incorporating CNTs into a ceramic matrix might be expected to produce a composite with both toughness and high-temperature stability.[7,8] However, there have been very few advances in CNT reinforced ceramic matrix composites because it is rather more difficult to fabricate a homogeneous dispersion of CNTs in a ceramic with strong interaction between CNTs and the matrix than to incorporate CNTs into a polymer.

The sol−gel technique is a well-known method for fabricating ceramic materials. One of the principal advantages in this method is that it permits the easy realization of doping profiles of nanoparticles homogeneously on a molecular scale.[9,10] Thus, it is currently used for preparing CNT reinforced ceramic oxide composites.[11−18] In most cases, however, the introduction of CNTs was realized by doping CNTs into an oxide sol or gel matrix,[11−15] or by doping CNTs into an oxide precursor solution.[16−18] Due to high viscousness of sol−gel and strong van der Waals attractive force among CNTs, it is very difficult to avoid the agglomeration of CNTs in the mixing sol or gel. Furthermore, weak interaction between CNTs and oxide sol−gel matrix would result in an inhomogeneous structure and degrade the hardness and strength of the ceramic. Therefore, from the application viewpoint, dispersing bundled CNTs to individual ones in a ceramic matrix and enhancing the interaction between CNTs and the matrix are both important scientific goals. However, studies on dispersing CNTs in oxide sol or gel are rarely reported.

In this paper, we report for the first time that multiwalled carbon nanotubes (MWCNTs) can be homogeneously dispersed and stabilized in TiO_2 sol via in situ sol−gel process. Our approach involves the use of oxidized MWCNTs, which can link with TiO_x generated from the hydrolysis and condensation of $Ti(OC_4H_9)_4$; by this the MWCNT (core)−TiO_2 (shell) tubular composite structures can be obtained. We expect that this simple route for preparing MWCNT−TiO_2 composites might open up new avenues not only in the fields of CNT−ceramic composites, but also in catalysts, optical devices, and biological sensing of oxides.

Experimental Section

The dispersion and functionalization experiments were carried out on oxidized MWCNTs. The detailed preparation process was as follows: (1) A 600 mg sample of commercially available MWNTs (purification >95%, average diameter <20 nm, chemical vapor deposition (CVD) method; Chengdu Organic Chemicals Co., Ltd., Chinese Academy of Sciences, China) was oxidized via sonication (with 15 W low-power base sonicator) in 80 mL of 1:3 (v:v) concentrated nitric acid−sulfuric acids at 60 °C for 10 h. The resultant solid was washed thoroughly with deionized water until about pH 6, collected, and dried in a vacuum at 40 °C. (2) A 14.0 mg sample of oxidized MWCNTs was dispersed in a mixture consisting of 10 mL of deionized water, 10 mL of anhydrous ethanol, and 2 mL of 70% HNO_3 under ultrasonic treatment for 10 min. Another solution consisting of 10 mL of $Ti(OC_4H_9)_4$ and 40 mL of anhydrous ethanol was then added dropwise into the above mixture at room temperature under rough stirring. After dropping and maintaining stirring for 3 h, a black-bluish sol was obtained. For comparison, we simultaneously prepared other two MWCNT−TiO_2 sols with the same concentration of MWCNTs: one was prepared from nonoxidized MWCNTs, and the other was prepared just through dispersing oxidized MWCNTs in pure TiO_2 sol, which will be explained in detail in the Results section. After the procedures, the suspensions were allowed to stand for several hours to 1 month. For the dispersion of oxidized MWCNTs in TiO_2 sol prepared through in situ sol−gel process,

* Corresponding author. Telephone: + 65 6790 6127. Fax: +65 6793 3318. E-mail address: xingbyan@yahoo.com.cn.

10.1021/jp065434g CCC: $33.50
Published on Web 12/02/2006

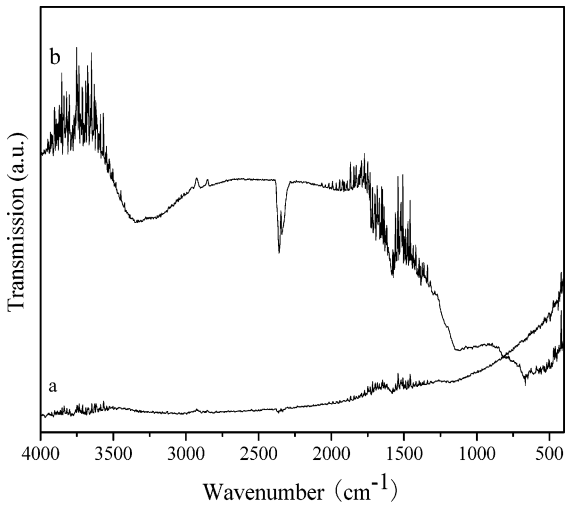

Figure 1. FTIR spectra of (a) pristine MWCNTs and (b) oxidized MWCNTs.

the MWCNTs were carefully collected by filtrating and subjected to further experiments if desired, including redispersing MWCNTs and annealing.

The nature of MWCNT surface groups before and after acid oxidization was investigated using an IFS3000 v/s Fourier transform infrared (FTIR) spectrometer. The microstructure of the functionalized MWCNTs was analyzed using transmission electron microscopy (TEM), X-ray photoelectron spectroscopy (XPS), and Raman spectroscopy. TEM images were obtained by a JEM-2010 instrument (JEOL), using an accelerating voltage of 200 kV. The XPS measurements were performed on a Perkin-Elmer PHI-5702 multifunctional X-ray photoelectron spectroscope (Physical Electronics, USA), using Mg Kα X-rays as the excitation source ($h\nu = 1253.6$ eV). The Raman spectra were recorded by a Renishaw Raman spectrometer (50 mW, 514.5 nm Ar^+ laser) at room temperature. The dispersion of MWCNTs was characterized by an atomic force microscope (AFM; Nanoscope III, Digital Instruments/Veeco Metrology Group, USA) and AFM images were obtained in tapping mode with standard Si/N tips. A clean silicon substrate was first covered with poly(dimethyldiallylammonium chloride) (PDDA, $M_w \approx$ 200 000−350 000; Aldrich) by dipping it in 1 wt % water solution for 10 min and washing with deionized water. A small drop of the dilute suspension of MWCNTs was then placed on the substrate and let dry at room temperature, followed by AFM imaging.

Results and Discussion

It is known that the chemical oxidation of carbon materials is frequently used as a method to obtain a more hydrophilic surface structure with a relatively large number of oxygen-containing surface groups. Previous reports[19−24] that referred to the oxidation of CNTs with nitric acid and sulfuric acid have suggested the introduction of many functional groups, such as hydroxyl (−OH), carboxyl (−COOH), and carbonyl (>C═O), on the surface of CNTs. In our experiments, the nature of the pristine and the oxidized MWCNT surface groups was investigated using FTIR spectroscopy (Figure 1). Compared to the spectrum of the pristine MWCNTs, the spectrum of the oxidized MWCNTs clearly shows the presence of oxygen-containing groups resulting from the oxidation: a broad band centered around 3346 cm^{-1} with a shoulder at 3213 cm^{-1} can be ascribed to O−H stretching vibrations in C−OH groups and water, respectively;[22,23] a band at 1721 cm^{-1} is attributed to C═O stretching vibrations in carboxyl and carbonyl groups;[20−24] a band at 1585 cm^{-1} and a weak shoulder at 1500−1357 cm^{-1} are assigned to O−H deformation vibrations; a broad band centered at 1153 cm^{-1} is associated with C−O stretching vibrations.[22]

The purpose of this study was to prepare stable suspensions of MWCNTs. We found that, in our experiments, after dispersing oxidized MWCNTs into water−ethanol−HNO_3 mixture under ultrasonic treatment for 1 h, the gravity-driven sedimentation of large MWCNT bundles was very fast and all of the MWCNTs settled at the bottom of the vial after several hours (Figure 2a). However, after adding $Ti(OC_4H_9)_4$−ethanol solution drop by drop, oxidized MWCNTs were homogeneously dispersed in the resulting sol and kept stable at least for 1 month, in which neither sedimentation nor aggregation of nanotube bundles was observed (Figure 2c). This indicates that oxidized MWCNTs can be protected by TiO_2 sol via in situ sol−gel process and hence supernatant MWCNTs become extremely stable at this stage. We are particularly concerned about the effect of oxidization of MWCNTs on the dispersing MWCNTs in TiO_2 sol. To detect this effect, this in situ sol−gel process was repeated with the pristine MWCNTs (14 mg). However, we found that, though the resultant dispersion was stable for initially several days, a small amount of precipitates was found at the bottom of the dispersion after 1 month (Figure 2b). The lighter color of this suspension compared to that of oxidized MWCNT−TiO_2 sol indicated that the oxidized MWCNTs have better dispersion in TiO_2 sol. This slow precipitation process might be driven by the gradual formation of large nanotube bundles through encountered discrete MWCNTs.

An attempt to directly disperse MWCNTs in pure TiO_2 sol confirmed the crucial importance of in situ sol−gel process. When the same mass (14 mg) of oxidized MWCNTs was mixed into the pure TiO_2 sol under ultrasonic treatment for 2 h, we found that the dispersion could not remain stable even for several hours. After 1 month, the color of suspension turned light blue and a layer of MWCNTs settled at the bottom of the vial (Figure 2d). Through comparing the color with that of pure TiO_2 sol (Figure 2e), we think that most of the oxidized MWCNTs were precipitated. Because the pure TiO_2 sol is a viscous suspension and there is strong van der Waals attractive force among MWCNTs, it would be very difficult to separate MWCNT bundles into individual MWCNTs even if the mixture had been sonicated for 2 h.

To fully understand the dispersion properties of MWCNTs in TiO_2 sol via in situ sol−gel process, it is important to investigate their microstructure and, in particular, the distribution of the MWCNTs within the sol matrix and the nature of the MWCNT−TiO_2 interface. Through dipping the sol suspension with copper grid and evaporating solvents, we were able to anchor the TiO_2 sol onto a copper grid and hence study the dispersion of MWCNTs by TEM. As seen in Figure 3a, the TEM micrograph of oxidized MWCNT−TiO_2 sol identified the presence of an individual MWCNT embedded within the matrix (arrow labeled), which implied that the MWCNTs were well separated in TiO_2 matrix and protected from aggregating with one another by TiO_2 sol. Moreover, we found that there was no obvious difference in the TEM pictures between the pristine and the oxidized MWCNT−TiO_2 topper suspension. However, when the two kinds of suspensions were filtrated, repeatedly ultrasonically washed with deionized water (in order to remove those TiO_2 precursor molecules without linking with MWCNTs), dried (at 80 °C), and prepared for TEM analyses, respectively, there was obvious difference existing between the TEM

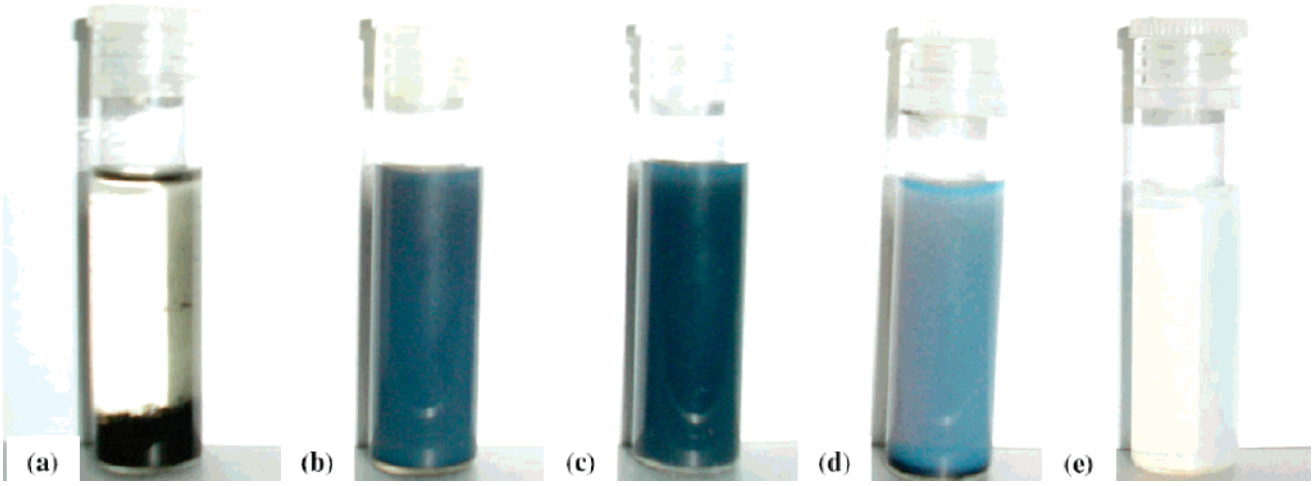

Figure 2. Optical micrographs of (1) oxidized MWCNTs dispersed in H_2O-HNO_3−ethanol solution, (b) pristine MWCNTs dispersed in TiO_2 sol via in situ sol−gel, (c) oxidized MWCNTs dispersed in TiO_2 sol via in situ sol−gel, (d) oxidized MWCNTs dispersed in TiO_2 sol via ultrasonic mixing, and (e) pure TiO_2 sol. The photo of sample a was taken after standing for 2 h, and the other samples were recorded after standing for 1 month.

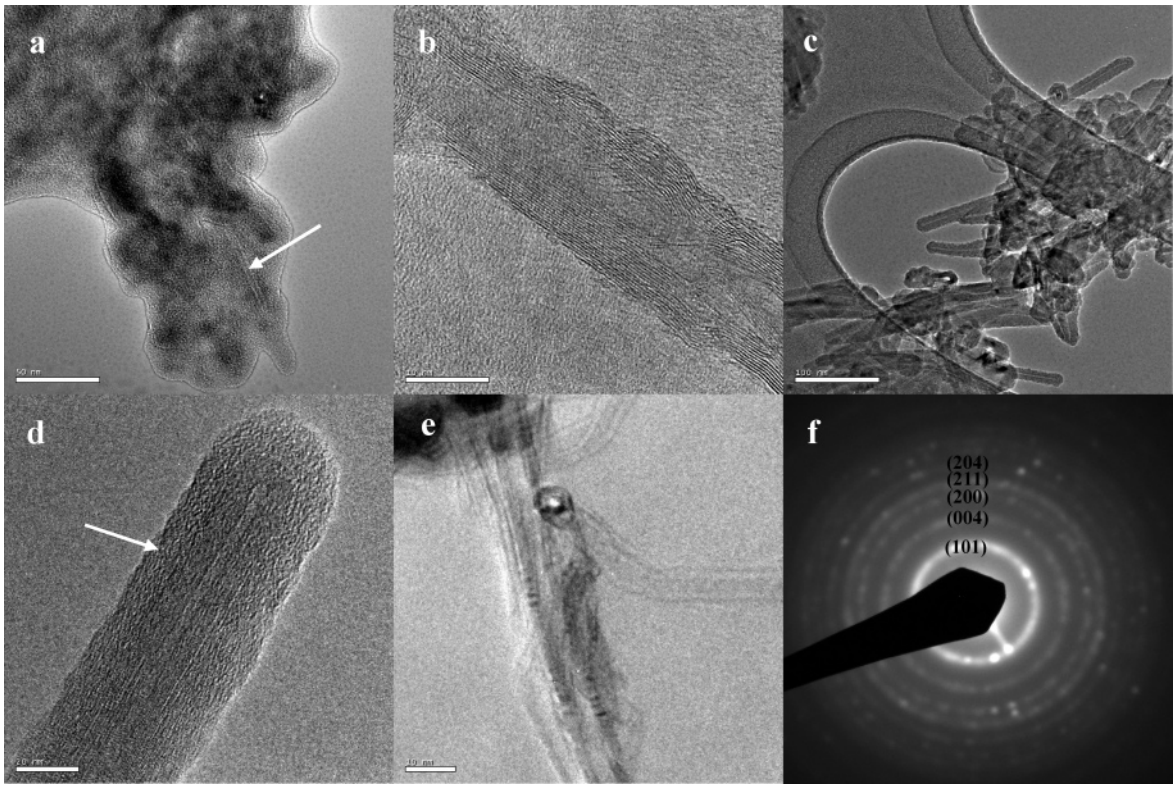

Figure 3. (a) TEM image of oxidized MWCNT−TiO_2 sol after drying; (b) TEM image of pristine MWCNT−TiO_2 sol after filtrating, washing, and drying; (c, d) TEM images of oxidized MWCNT−TiO_2 sol after filtrating, washing, and drying; (e) TEM image of oxidized MWCNT−TiO_2 sol after filtrating, washing, drying, and annealing at 700 °C; (f) corresponding SAED pattern of nanotubes shown in (e). Inset scale bar: (a) 50, (b) 10, (c) 100, (d) 20, and (e) 10 nm.

micrographs. For the sample prepared from the pristine MWCNT−TiO_2 sol, high-resolution TEM indicated that MWCNT was highly graphitic with layers parallel to the tube axis and was not coated with TiO_x material on its outer layer surface (Figure 3b). In contrast, for the sample prepared from the oxidized MWCNT−TiO_2 sol, low-magnification TEM showed a homogeneous sample with some nanotubes (Figure 3c). Furthermore, higher magnification showed that every nanotube surface was coated with a uniform amorphous TiO_x layer (arrow labeled), which indicated there was strong interaction existing between the oxidized MWCNT and TiO_x layer (Figure 3d). Themogravimetric analysis (TGA) revealed that the MWCNTs were completely oxidized at 610 °C, leaving a residue of 10 wt %. Thus, via heat treatment of the TiO_x-coated MWNTs at 700 °C for 1 h in air atmosphere (heating rate 25 °C/min), the MWCNTs were oxidized, yielding the TiO_2 tubular nanostructures shown in the TEM image in Figure 3e. The corresponding selected area electron diffraction (SAED) pattern shown in Figure 3f revealed that the structural nature corresponded to TiO_2 crystalline phase. Based on the TEM analytical results,

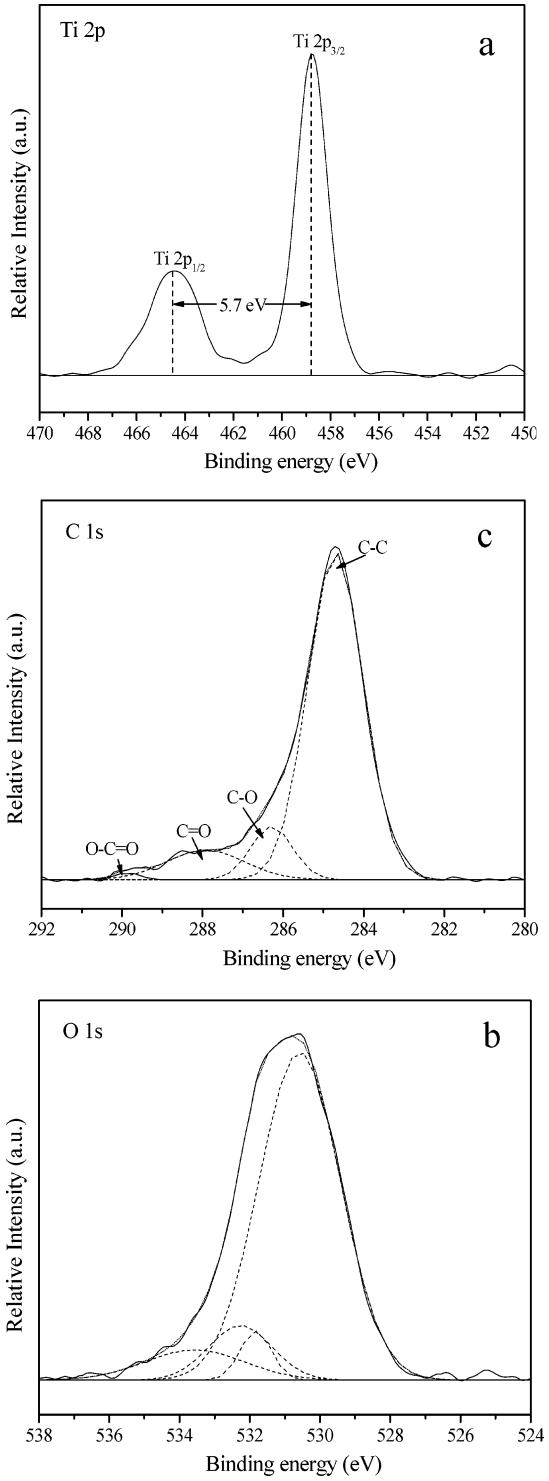

Figure 4. Ti 2p (a), O 1s (b), and C 1s (c) core level XPS spectra of TiO_x-wrapped MWCNT sample.

we conclude that, although pristine MWCNTs can be dispersed by TiO_2 sol via the in situ sol−gel process to a certain extent, there is no strong interaction existing between this kind of MWCNTs and TiO_2 sol. In contrast, via in situ sol−gel process, oxidized MWCNTs can be synchronously well-dispersed and functionalized by TiO_2 sol.

XPS measurements were carried out to study the chemical state of the Ti compounds. Figure 4 shows the XPS data for Ti, O, and C core levels with a sample of the dried (at 80 °C) functionalized MWCNT powder. The formation of the TiO_x on the sidewall surface of the oxidized MWCNTs is shown clearly by the Ti 2p XPS data in Figure 4a, which shows the core-level spectral values comparable to bulk TiO_2;[25] i.e., the Ti 2p 3/2 peak is at 458.8 eV and the Ti 2p 3/2 and 1/2 spin−orbital splitting is 5.7 eV. Moreover, the O/Ti atomic ratio is calculated to be about 2.3, which is slightly higher than that of 2 given from pure TiO_2. It may be because partial oxygen is assigned from the oxidized MWCNTs. Figure 4 also shows the corresponding high resolution and curve fittings of O 1s and C 1s spectra of the same sample. It is found that the O 1s spectrum of the as-prepared sample (Figure 4b) can be fitted to four peaks. The main peak at 530.6 eV is assigned to oxygen from TiO_x. The other three peaks in the shoulder of the main peak with high binding energies located at 531.8, 532.3, and 533.6 eV are attributed to carbonyl, phenol, and carboxyl groups, respectively.[26] Similarly, the C 1s peaks can be fitted to a peak of graphite and three other peaks (Figure 4c). The peak of typical graphitic carbon at 284.7 eV represents the C 1s binding energy of the MWCNTs. The three peaks in the shoulder of the main peak with higher binding energies located at 286.3, 287.9, and 289.9 eV can be assigned to C−O, C═O, and COO− species, respectively.[27−29] These results provide further evidence that oxygen-based functional groups were introduced to the nanotube surface.

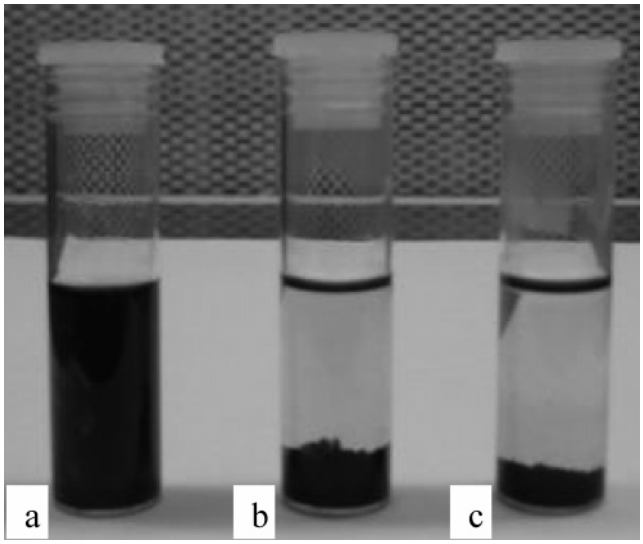

Figure 5. Optical micrographs of TiO_x-wrapped MWCNTs that were dissolved in ethanol (a), THF (b), and toluene (c), respectively. All pictures were taken after standing for 1 h.

The freshly prepared amorphous TiO_x-wrapped MWCNT powder through filtering and washing was redispersed in several liquids. The results reveal that the functionalized MWCNTs are easily dispersed in some polar liquid containing the hydroxyl group, such as water and ethanol. For example, the functionalized MWCNTs' solubility in ethanol is about 0.2 mg/mL (Figure 5a). We believe that the solubilization is closely connected with the existence of some Ti−OH groups on the surface of the as-prepared functionalized MWCNTs. However, this kind of MWCNT cannot be soluble in other common organic solvents such as tetrahydrofuran (THF) and toluene (Figure 5b,c) even after ultrasonic treatment for 1 h. It is well-known that organic titanates can be soluble in THF and toluene. If MWCNTs were coated with amorphous organic titanate instead of amorphous TiO_x during the in situ sol−gel process, the resulting functionalized MWCNTs would be soluble in THF and toluene. Consequently, the majority of Ti in the as-prepared samples in our experiment is not organic titanate. More importantly, to our knowledge, this represents the first observation of significant dissolution of TiO_x-coated MWCNTs in aqueous and alcoholic solvents, which would provide an efficient

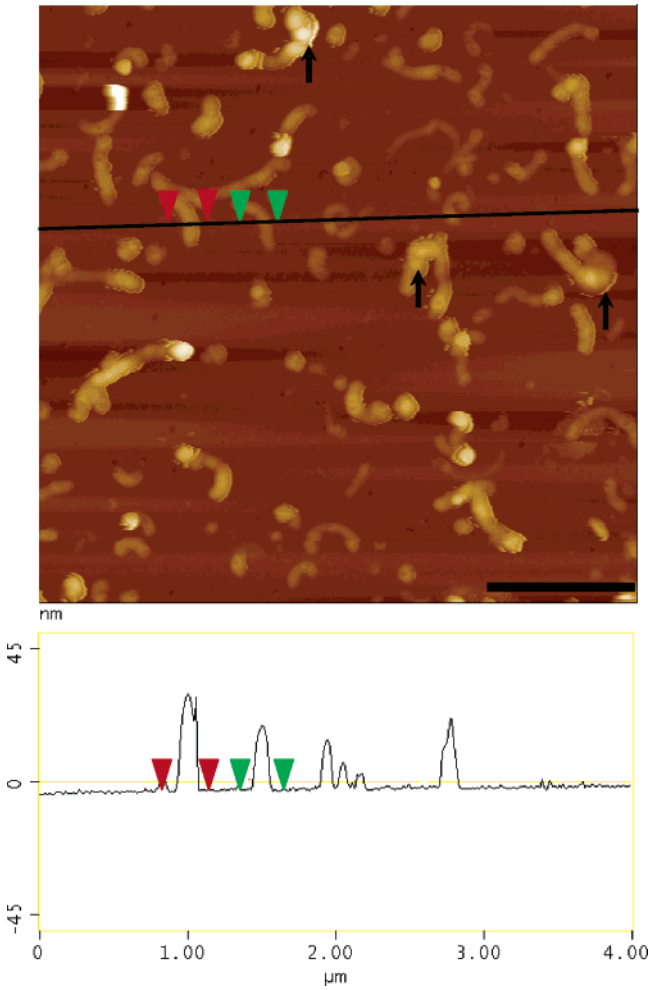

Figure 6. AFM height image and section analysis of TiO_x-wrapped MWCNTs that were dissolved in ethanol and dispersed on a PDDA/silicon surface.

method for fabricating highly uniformed CNT−oxide nanocomposites or films.

The dispersion state of oxidized MWCNTs was further characterized by AFM. A very dilute suspension of the functionalized MWCNTs in ethanol (0.001 mg/mL) was prepared for AFM investigation. The aim of this procedure was to provide a clearer representation of nanotubes on AFM images. According to previously developed surface modification approaches,[30,31] we were able to anchor the above MWCNT suspension onto PDDA-functionalized Si surface and hence study the dispersed MWCNTs. We found experimentally that the PDDA cushion put on the Si substrate for AFM imaging made the surface very hydrophilic and resulted in a more uniform spreading of water droplets containing nanotubes. According to AFM data (Figure 6), most of the MWCNTs are individual and well separated from each other, with the length being $<1\ \mu$m. Most importantly, section analysis indicated that the majority of MWCNTs are large in diameter compared to the pristine MWCNTs, which can be seen from the section analysis of the corresponding AFM image: the height of the two nanotube-like objects marked with red and green labels, respectively, is about 35 and 24 nm, which all are larger than the diameter of pristine MWCNTs (less than 20 nm). The increase of the diameter implies that the MWCNTs are wrapped with a thin coating, in this case TiO_x film. It should be demonstrated that some "huge" tubes (black arrows labeled) can be seen in the AFM image. Deriving from the diversity in

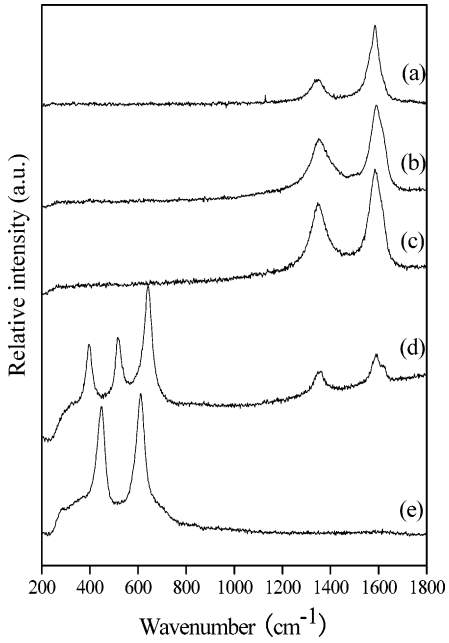

Figure 7. Raman spectra of pristine MWCNTs (a), oxidized MWCNTs (b), and oxidized MWCNT−TiO_x core/shell structural composite before (c) and after annealing in air at 500 (d) and 800 °C (e), respectively.

the color contrast and the difference in the diameter, we believe that a few granular nanoparticles are aggregated on the surface of the MWCNTs to form these uneven tubes. It may be due to the following reason: there are some defects existing on the surface of the pristine MWCNTs and these sites with defects would take higher density COOH and OH acid groups after the oxidization process; then higher density TiO_x would be linked on these special sites during the in situ sol−gel process; consequently, the TiO_x would not appear to be distributed uniformly along the nanotube surface and some granular nanoparticles would form on the special sites. Of course, such aggregates on the surface might arise during the drying process as well.[32] Moreover, a number of spherical nanoparticles also can be observed, which probably correspond to TiO_x micelles.

The functionalized MWCNT powder through filtering, washing, and drying was annealed at 500 and 800 °C in air atmosphere for 1 h. The Raman spectra of pristine MWCNTs, oxidized MWCNTs, and MWCNT−TiO_x composites before and after annealing are shown in Figure 7. It is clear that the peaks in Figure 7b,c are similar to the ones observed for pristine MWCNTs (Figure 7a) except that the ratio of the peak intensity changes, which is due to the oxidization of MWCNTs. The strong peak at 1585 cm^{-1} (G lines) is the Raman-allowed phonon high-frequency E_{2g} first-order mode, and the disorder-induced peak at 1347 cm^{-1} (D lines) may originate from defects in the curved graphene sheets, tube ends, and turbostratic structure.[33,34] However, after annealing, the Raman spectra show the obvious difference: after annealing at 500 °C (Figure 7d), three new peaks at 367, 515, and 640 cm^{-1} appeared, which are attributed to the anatase phases of TiO_2 crystal; for the sample after annealing at 800 °C (Figure 7e), however, two new peaks at 447 and 613 cm^{-1} appeared, which are attributed to the rutile phases of TiO_2 crystal.[35] Moreover, because the MWCNTs were completely oxidized above 610 °C revealed by TGA, the D line and G line of MWCNTs disappeared in the Raman spectrum in Figure 7e.

It is well-known that the sol−gel synthesis of metal oxides is based on the polycondensation of metal alkoxides $M(OR)_z$ in which R is usually an alkyl group (R = CH_3, C_2H_5, ...) and

z is the oxidation state of the metal atom M^{z+}. The sol−gel chemistry involves two steps:[36] or

(i) hydrolysis for the formation of reactive M−OH groups:

$$M-OR + H_2O \rightleftharpoons M-OH + ROH \quad (1)$$

(ii) condensation leading to the formation of bridging oxygen:

$$M-OH + RO-M \rightleftharpoons M-O-M + ROH \quad (2)$$

$$M-OH + HO-M \rightleftharpoons M-O-M + H_2O \quad (3)$$

Transition metal alkoxides are usually highly reactive toward hydrolysis, which easily takes place with a very small amount of water.[36] Because the amount of water used in our paper is superfluous, the hydrolysis of every drop of $Ti(OC_4H_9)_4$ must be fast and entire. In other words, the hydrolysis reaction must take place first and form the hydroxide of the titanium, $Ti(OH)_4$. We believe that the dispersion of MWCNTs must be closely connected to the subsequent chemical activities of the $Ti(OH)_4$. Consequently, the most likely dispersion mechanism is expected as followed: Some gaps may exist among bounded MWCNTs to allow the $Ti(OH)_4$ molecules to insert into such gaps. During the condensation process (eq 3), the growing $Ti(OH)_4$ chain in the gaps would wedge away the MWCNT bundles and then break down the bundles into individual MWCNTs. Moreover, the Ti−OH groups take some negative charges in acid solution, and then charge repulsion originating from these negatively charged Ti−OH species would favor the dispersion of MWCNTs. Thus, MWCNTs are uniformly and individually dispersed in the resulting TiO_2 sol. For oxidized MWCNTs, the formation mechanism of MWCNT−TiO_x composites with the tubular nanostructure is believed to involve chemical interaction between the carboxylic and hydroxyl groups of oxidized MWCNTs and the Ti−OH group of $Ti(OH)_4$ during the in situ sol−gel process. This chemical interaction is very similar to the one that has been demonstrated by Li[37] and Rao,[38] respectively. In our experiments, superfluous water and fast-thorough hydrolysis reaction of $Ti(OC_4H_9)_4$ result in an amorphous TiO_x layer instead of an organic titanate layer being coated on the MWCNTs' surfaces.

Conclusion

In summary, we have demonstrated that MWCNTs can be homogeneously dispersed and stabilized by TiO_2 sol via in situ sol−gel process. Furthermore, during the hydrolysis and condensation process originating from $Ti(OC_4H_9)_4$, the oxidized MWCNTs can be coated with an amorphous TiO_x thin layer; thus MWCNT (core)−TiO_x (shell) tubular composite structures and crystal TiO_2 nanotubes can be obtained. This method is potentially useful as an efficient route to prepare homogeneous CNT−ceramic composites. Moreover, the strategy is readily extended to generate a heterojunction incorporating CNT and nanostructural oxides.

Acknowledgment. The authors acknowledge support from the Singapore Millennium Foundation.

References and Notes

(1) Coleman, J. N.; Khan, U.; Gun'ko, Y. K. *Adv. Mater.* **2006**, *18*, 689−706.

(2) Jonghwan, S.; Nikhil, K.; Pawel, K. K.; Pulickel, A. *Nat. Mater.* **2005**, *4*, 134−137.

(3) Ajayan, P. M.; Shadler, L. S.; Giannaris, C.; Rubio, A. *Adv. Mater.* **2000**, *12*, 750−753.

(4) Wagner, H. D.; Lourie, O.; Feldman, Y.; Tenne, R. *Appl. Phys. Lett.* **1998**, *72*, 188−190.

(5) Kovtyukhova, N. I.; Mallouk, T. E. *J. Phys. Chem. B* **2005**, *109*, 2540−2545.

(6) Pradhan, B.; Batabyal, S. K.; Pal, A. J. *J. Phys. Chem. B* **2006**, *110*, 8274−8277.

(7) Zhan, G. D.; Kuntz, J. D.; Wan, J. *Nat. Mater.* **2003**, *2*, 38−42.

(8) Zhan, G. D.; Kuntz, J. D.; Garay, J. E. *Appl. Phys. Lett.* **2003**, *83*, 1228−1230.

(9) Yang, H.; Yao, X.; Wang, X.; Xie, S.; Fang, Y.; Liu, S.; Gu, X. *J. Phys. Chem. B* **2003**, *107*, 13319−13322.

(10) Ferrer, M. L.; Monte, F. *J. Phys. Chem. B* **2005**, *109*, 80−86.

(11) Berguiga, L.; Bellessa, J.; Vocanson, F.; Bernstein, E.; Plenet, J. C. *Opt. Mater.* **2006**, *28*, 167−171.

(12) Vincent, P.; Brioude, A.; Journet, C.; Rabaste, S.; Purcell, S. T.; Le Brusq, J.; Plenet, J. C. *J. Non-Cryst. Solids* **2002**, *311*, 130−137.

(13) Vasilis, G.; Gavalas, R. A.; Dibakar, B.; Leonidas, G. B. *Nano Lett.* **2001**, *1*, 719−721.

(14) Mo, C. B.; Cha, S. I.; Kim, K. T.; Lee, K. H.; Hong, S. H. *Mater. Sci. Eng., A* **2005**, *395*, 124−128.

(15) Jitianu, A.; Cacciaguerra, T.; Benoit, R.; Delpeux, S.; Beguin, F.; Bonnamy, S. *Carbon* **2004**, *42*, 1147−1151.

(16) Álvaro, M.; Atienzar, P.; Bourdelande, J. L.; García, H. *Chem. Commun.* **2002**, 3004−3005.

(17) Norifumi, F.; Masayoshi, A.; Taketomo, Y.; Seiji, S. *J. Mater. Chem.* **2004**, *14*, 2106−2114.

(18) Seeger, T.; Köhler, T.; Frauenheim, T.; Grobert, N.; Rühle, M.; Terrones, M.; Seifert, G. *Chem. Commun.* **2002**, 34−35.

(19) Jia, Z.; Wang, Z.; Liang, J.; Wei, B.; Wu, D. *Carbon* **1999**, *37*, 903−906.

(20) Shaffer, M. S. P.; Fan, X.; Windle, A. H. *Carbon* **1998**, *36*, 1603−1612.

(21) Chen, J.; Hamon, M. A.; Hu, H.; Chen, Y.; Rao, A. M.; Eklund, P. C.; Haddon, R. C. *Science* **1998**, *282*, 95−98.

(22) Kovtyukhova, N. I.; Mallouk, T. E.; Pan, L.; Dickey, E. C. *J. Am. Chem. Soc.* **2003**, *125*, 9761−9769.

(23) Li, Y. H.; Xu, C.; Wei, B.; Zhang, X.; Zheng, M.; Wu, D.; Ajayan, P. M. *Chem. Mater.* **2002**, *14*, 483−485.

(24) Yu, R.; Chen, L.; Liu, Q.; Lin, J.; Tan, K.-L.; Ng, S. C.; Chan, H. S. O.; Xu, G.-Q.; Hor, S. T. A. *Chem. Mater.* **1998**, *10*, 718−722.

(25) Wagner, C. D.; Riggs, W. M.; Davis, L. E.; Moulder, J. F.; Muilenberg, G. E. *Handbook of X-ray Photoelectron Spectroscopy*; Perkin-Elmer: Wellesley, MA, 1978.

(26) Fang, H. T.; Liu, C. G.; Liu, C.; Li, F.; Liu, M.; Cheng, H. M. *Chem. Mater.* **2004**, *16*, 5744−5750.

(27) Ago, H.; Kugler, T.; Cacialli, F.; Salaneck, W. R.; Shaffer, M. S. P.; Windle, A. H. *J. Phys. Chem. B* **1999**, *103*, 8116−8121.

(28) Kovtyukhova, N. I.; Mallouk, T. E.; Pan, L.; Dickey, E. C. *J. Am. Chem. Soc.* **2003**, *125*, 9761−9769.

(29) Bond, A. M.; Miao, W.; Raston, C. L. *Langmuir* **2000**, *16*, 6004−6012.

(30) Sinani, V. A.; Gheith, M. K.; Yaroslavov, A. A.; Rakhnyanskaya, A. A.; Sun, K.; Mamedov, A. A.; Wicksted, J. P.; Kotov, N. A. *J. Am. Chem. Soc.* **2005**, *127*, 3463−3472.

(31) Zhu, J.; Yudasaka, M.; Zhang, M. F.; Iijima, S. *J. Phys. Chem. B* **2004**, *108*, 11317−11320.

(32) Pender, M. J.; Sowards, L. A.; Hartgerink, J. D.; Stone, M. O.; Naik, R. R. *Nano Lett.* **2006**, *6*, 40−44.

(33) Tan, P. H.; Zhang, S. L.; Yue, K. T.; Huang, F.; Shi, Z.; Zhou, X.; Gu, Z. *J. Raman Spectrosc.* **1997**, *28*, 369−372.

(34) Hiura, H.; Ebbesen, T. W.; Tanigaki, K.; Takahashi, H. *Chem. Phys. Lett.* **1993**, *202*, 509−512.

(35) Wang, W.; Gu, B.; Liang, L.; Hamilton, W. A.; Wesolowski, D. J. *J. Phys. Chem. B* **2004**, *108*, 14789−14792.

(36) Livage, J.; Ganguli, D. *Sol. Energy Mater. Sol. Cell* **2001**, *68*, 365−381.

(37) Li, X. H.; Niu, J. L.; Zhang, J.; Li, H. L.; Liu, Z. F. *J. Phys. Chem. B* **2003**, *107*, 2453−2458.

(38) Gomathi, A.; Vivekchand, S. R. C.; Govindaraj, A.; Rao, C. N. R. *Adv. Mater.* **2005**, *17*, 2757−2761.